© 2015. Published by The Company of Biologists Ltd | Development (2015) 142, 2425-2430 doi:10.1242/dev.121996

RESEARCH REPORT

A trans-homologue interaction between reciprocally imprinted *miR-127* and *Rtl1* regulates placenta development

Mitsuteru Ito[1], Amanda N. Sferruzzi-Perri[2], Carol A. Edwards[1], Bjorn T. Adalsteinsson[1], Sarah E. Allen[1], Tsui-Han Loo[3], Moe Kitazawa[4], Tomoko Kaneko-Ishino[5], Fumitoshi Ishino[4], Colin L. Stewart[3] and Anne C. Ferguson-Smith[1,2,*]

ABSTRACT

The paternally expressed imprinted retrotransposon-like 1 (*Rtl1*) is a retrotransposon-derived gene that has evolved a function in eutherian placentation. Seven miRNAs, including *miR-127*, are processed from a maternally expressed antisense *Rtl1* transcript (*Rtl1as*) and regulate *Rtl1* levels through RNAi-mediated post-transcriptional degradation. To determine the relative functional role of *Rtl1as* miRNAs in *Rtl1* dosage, we generated a mouse specifically deleted for *miR-127*. The *miR-127* knockout mice exhibit placentomegaly with specific defects within the labyrinthine zone involved in maternal-fetal nutrient transfer. Although fetal weight is unaltered, specific *Rtl1* transcripts and protein levels are increased in both the fetus and placenta. Phenotypic analysis of single (Δ*miR-127*/*Rtl1* or *miR-127*/Δ*Rtl1*) and double (Δ*miR-127*/Δ*Rtl1*) heterozygous *miR-127*- and *Rtl1*-deficient mice indicate that *Rtl1* is the main target gene of *miR-127* in placental development. Our results demonstrate that *miR-127* is an essential regulator of *Rtl1*, mediated by a trans-homologue interaction between reciprocally imprinted genes on the maternally and paternally inherited chromosomes.

KEY WORDS: Genomic imprinting, Rtl1 (Peg11), miR-127, *Mir127*, Placenta development

INTRODUCTION

Mammalian genomic imprinting is an epigenetic process whereby genes are mono-allelically expressed in a parent-of-origin-specific manner (Ferguson-Smith, 2011). The imprinted gene cluster on mouse chromosome 12 contains four paternally expressed protein-coding genes and maternally expressed non-coding RNAs (Fig. 1A) (da Rocha et al., 2008). One of these paternally expressed genes, retrotransposon-like 1 (*Rtl1*; also known as *Peg11*), is derived from a Ty3/Gypsy-type retrotransposon that in eutherians has evolved a large conserved open reading frame (ORF) but has lost its long terminal repeats (LTRs), resulting in loss of the original retroviral promoter activity (Brandt et al., 2005; Youngson et al., 2005; Edwards et al., 2008).

The primary antisense *Rtl1* transcript (*Rtl1as*) is exclusively expressed from the maternally inherited *Rtl1* locus but in the opposite direction to *Rtl1* (Fig. 1A) (Seitz et al., 2003). At least seven microRNAs (miRNAs) processed from *Rtl1as* are therefore perfectly complementary in sequence to *Rtl1* (Davis et al., 2005). Maternally inherited deletion of the differentially methylated imprinting control region for the locus (IG-DMR) causes a maternal-to-paternal epigenotype switch across the whole imprinted gene cluster (Lin et al., 2003). This is associated with repression of all the maternally expressed non-coding RNAs, including the miRNAs, and inappropriate activation of the usually paternally expressed protein-coding genes on the maternally inherited chromosome, resulting in a double dose. However, *Rtl1* mRNA levels increase 4.5-fold from both alleles, instead of the double dose expected from loss of imprinting (LOI). This suggests that the increase in *Rtl1* dosage in the mutant is the cumulative effect of both LOI and a failure to destabilise the now biallelically expressed transcript by the antisense miRNAs (Lin et al., 2003). Further evidence that these miRNAs can degrade *Rtl1* transcripts by the RNAi machinery *in vivo* came from the identification of both DROSHA and DICER cleavage products for each of the miRNAs (Davis et al., 2005). Previous work has shown that *Rtl1* gene deletion causes growth retardation of both the fetus and placenta and that removal of six of the seven miRNAs on *Rtl1as* leads to *Rtl1* overproduction and placentomegaly (Sekita et al., 2008).

Further findings indicate that *miR-127* on *Rtl1as* can be independently regulated in human cancer (Iorio et al., 2005; Lu et al., 2005), and that on its own *miR-127* may be the major contributor to *Rtl1* silencing in differentiating mouse embryonic stem cells (ESCs) (Ciaudo et al., 2009). These findings suggest that *miR-127* might play a prominent role in controlling *Rtl1* dosage during normal development. In order to clarify the biological significance of *miR-127*, we generated *miR-127* (*Mir127*) knockout mice and studied its impact on *Rtl1* transcript and protein levels and consequences for placental development.

RESULTS AND DISCUSSION

Maternal *miR-127* deletion induces placentomegaly

The schematic organisation of the imprinted *Rtl1* sense and antisense transcripts is shown in Fig. 1A. A 134 bp deletion removed *miR-127* upon maternal transmission (Δ*miR-127*), while the same deletion when paternally transmitted (Δ*Rtl1*) introduces a nonsense mutation in the third exon of *Rtl1*, resulting in premature translation termination of a normally transcribed mutant transcript (Fig. 1A; supplementary material Fig. S1B). Western blotting data showed no detectable RTL1 protein in Δ*Rtl1* conceptuses (supplementary material Fig. S1G), although *Rtl1* mRNA was stable (supplementary material Fig. S3A). All phenotypic analyses were carried out on the C57BL/6J background unless otherwise indicated.

[1]Department of Genetics, University of Cambridge, Cambridge CB2 3EH, UK. [2]Centre for Trophoblast Research, Department of Physiology, Development, and Neuroscience, University of Cambridge, Cambridge CB2 3EG, UK. [3]Laboratory of Developmental and Regenerative Biology, Institute of Medical Biology, 8A Biomedical Grove, Immunos, Singapore 138648. [4]Department of Epigenetics, Medical Research Institute, Tokyo Medical and Dental University, 1-5-45 Yushima, Bunkyo-ku, Tokyo 113-8510, Japan. [5]School of Health Sciences, Tokai University, 143 Shimokasuya, Isehara, Kanagawa 259-1193, Japan.

*Author for correspondence (afsmith@mole.bio.cam.ac.uk)

Received 12 January 2015; Accepted 8 June 2015

Development (2015) 142, 2425-2430 doi:10.1242/dev.121996

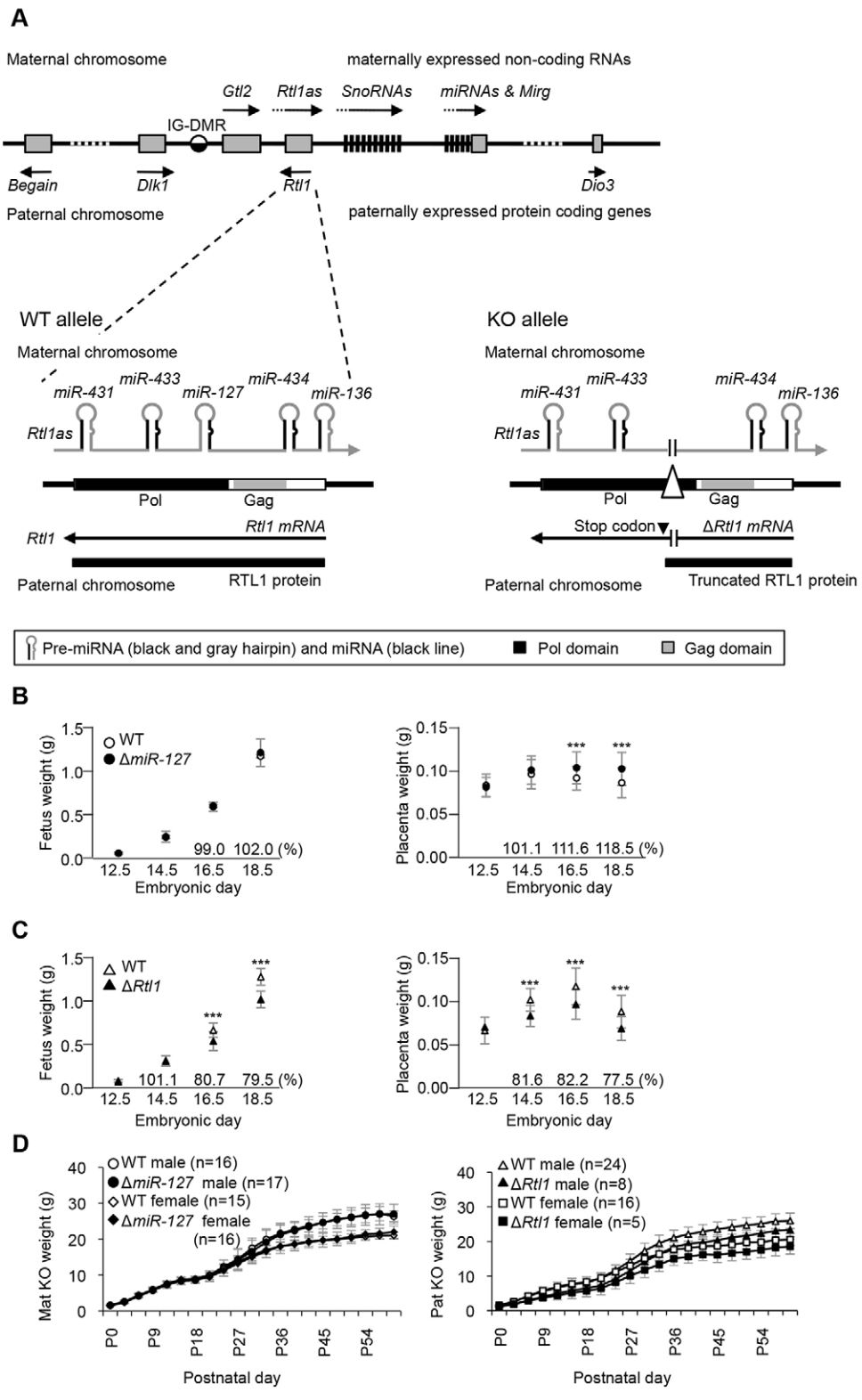

Fig. 1. Structure of the *Rtl1* locus and pre- and postnatal growth of *miR-127* and *Rtl1* knockout mice. (A) Schematic presentation of the mouse *Dlk1-Dio3* cluster. (Lower left) The WT *Rtl1* locus (exon 3). *Rtl1* is expressed from the paternal chromosome and *Rtl1as* is exclusively transcribed from the maternal chromosome. (Lower right) The knockout (KO) allele. The paternally transmitted deletion introduces an in-frame stop codon that results in premature termination of RTL1. The maternally transmitted deletion lacks *miR-127* expression. (B,C) Prenatal growth of Δ*miR-127* mice and Δ*Rtl1* mice, respectively. Left and right panels show embryonic and placental growth curves in mutant and WT littermates from E12.5 to E18.5. All embryos and placentas were collected from the N6 and N7 generation. (D) Postnatal growth curve of Δ*miR-127* (left) and Δ*Rtl1* (right) from birth to 2 months. Weights were measured every 3 days. Δ*Rtl1* mice were significantly smaller than WT. ***P<0.005 (Student's t-test). Error bars indicate s.d.

Placentae were significantly overgrown in Δ*miR-127* mutants, which was first apparent at E16.5; placental weights were 111.6% and 118.5% compared with wild type (WT) at E16.5 and E18.5, respectively (Fig. 1B). By contrast, there was no effect of Δ*miR-127* on fetal weight during development (Fig. 1B). Previous work had shown that when six miRNAs, including *miR-127*, are deleted, mutant placental weights are 156% of WT values at E18.5, although fetal weights are not different (Sekita et al., 2008). These data suggest that *miR-127* functions to suppress placental growth in pregnancy, although placentomegaly in Δ*miR-127* was milder than with the larger deletion encompassing six miRNAs. After birth, the Δ*miR-127* mice grew at comparable rates to WT and no lethality was observed either pre- or postnatally in these mice (Fig. 1D; supplementary material Tables S1 and S2).

Δ*Rtl1* mice showed prenatal growth retardation starting at E16.5; fetal weights were ∼80% of WT (Fig. 1C). Mice have reduced wet

Development (2015) 142, 2425-2430 doi:10.1242/dev.121996

weight at birth (~70% of WT) and remain growth retarded into adulthood (Fig. 1D). Prenatally, the placenta is growth restricted from E14.5, prior to the onset of fetal growth restriction, suggesting a causal role for the placenta in the fetal growth phenotype (Fig. 1C). Prenatal lethality was not observed in Δ*Rtl1* but the majority of neonates died within 1 day of birth (supplementary material Tables S1 and S2). In situations in which Δ*Rtl1* newborns survived more than 2 days, animals survived to adulthood. The lethality of Δ*Rtl1* was not evident on a mixed 129aa and C57BL/6J background (supplementary material Table S1). The embryonic lethality we report differs from that associated with the previously reported larger deletion, where lethality occurred during gestation upon paternal transmission (Sekita et al., 2008), despite both mutants lacking the RTL1 protein.

Δ*miR-127* causes defects in the placental labyrinthine zone

Placental structure was analysed stereologically (Gundersen et al., 1988; Mandarim-de-Lacerda, 2003; Coan et al., 2004) upon both maternal and paternal transmission of the deletion at E18.5. In Δ*miR-127* the labyrinthine zone (Lz), which is the site of nutrient and gaseous exchange between the maternal and fetal blood supplies, was expanded (142.3% of WT; Fig. 2A,C). Conversely, the volume of the Lz was reduced in Δ*Rtl1* (64.7% of WT; Fig. 2B,D). In contrast to the Lz, the junctional zone, decidual basalis and chorion were all unaffected by *miR-127* or *Rtl1* deficiency.

Detailed structural analysis of the Lz showed that both the fetal capillaries (FCs) and the labyrinthine trophoblast (LT) were significantly increased in Δ*miR-127*, with a non-significant trend for expanded maternal blood spaces (MBSs) (Fig. 2E; supplementary material Fig. S2). Similar to the volume differences, the surface areas of FCs and MBSs were also extended in Δ*miR-127* (supplementary material Table S3). Moreover, the average length of FCs in the Lz was increased in Δ*miR-127*, without a change in diameter. There was no effect of *miR-127* deficiency on the thickness of the interhemal trophoblast membrane, where nutritional exchange takes place. These results suggest that *miR-127* suppresses fetal capillarisation of the placental exchange region.

In Δ*Rtl1*, placental abnormalities were observed in the same compartments affected by *miR-127* deficiency, but with opposite phenotypes (Fig. 2F; supplementary material Fig. S2). These results suggest that *Rtl1* supports FC elongation and that the two genes interact to regulate the same placental processes. The alterations in MBS and FC surface area would affect nutrient and oxygen supply to the fetus and contribute to the observed fetal growth restriction. The theoretical diffusion capacity (TDC) and specific diffusion capacity (SDC) are barometers for the potential ability of small molecules such as oxygen to transfer by passive diffusion from mother to fetus (Laga et al., 1973). The TDC and SDC values of the mutant placentae indicate that Δ*miR-127* mice have a higher diffusive capacity than WT and, conversely, that Δ*Rtl1* placentae have a reduced capacity (supplementary material Table S3). Although this is likely to contribute to the growth retardation of the Δ*Rtl1* fetuses, it is noteworthy that the Δ*miR-127* mutants are not growth enhanced. Previous work has proposed that *Rtl1* cleaves an extracellular matrix (ECM) component resulting in a release of growth factors to promote hepatocarcinogenesis (Riordan et al., 2013). During

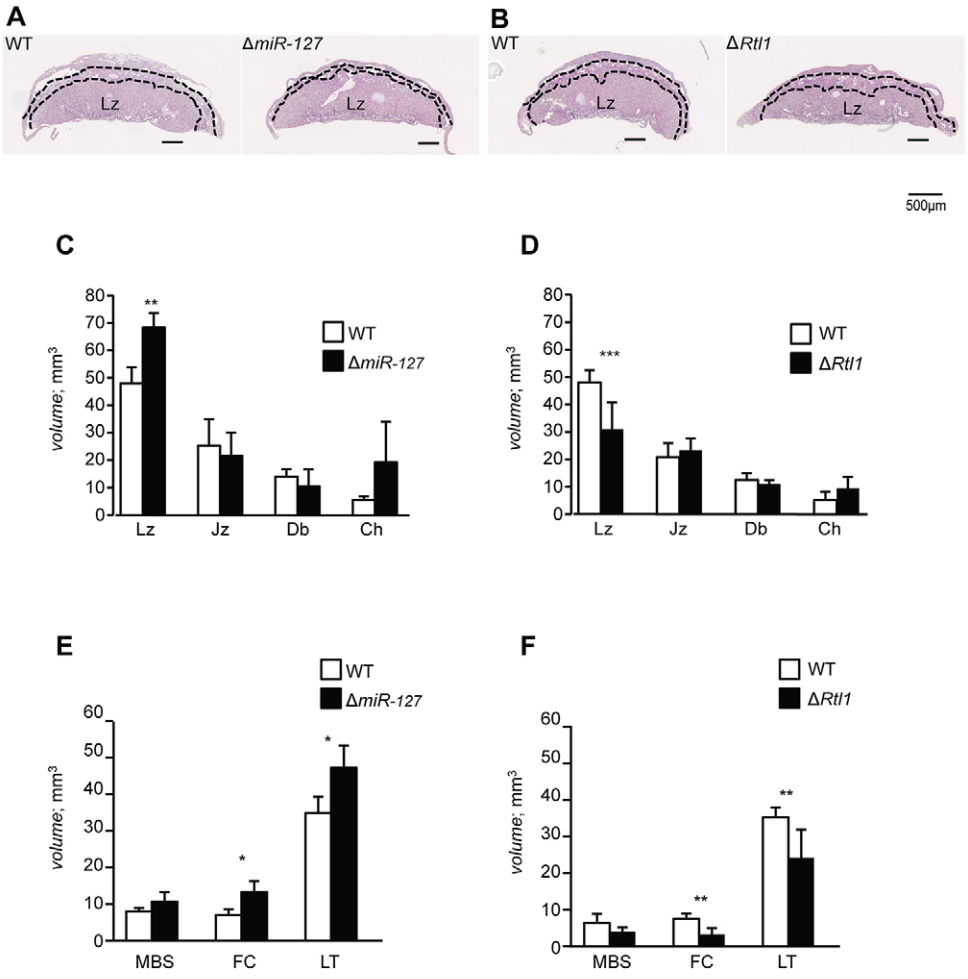

Fig. 2. Histological analysis shows abnormality in the labyrinthine zone in Δ*miR-127* and Δ*Rtl1*. (A,B) Histological analysis of WT littermate and Δ*miR-127* or Δ*Rtl1*, respectively. H&E-stained paraffin sections of E18.5 placentae. Dashed lines demarcate Lz (bottom layer), Jz (middle layer) and Db (top layer). Scale bars: 500 μm. (C-F) The volumes of placental and labyrinthine compartments in WT, Δ*miR-127* and Δ*Rtl1*. Lz, labyrinthine zone; Jz, junctional zone; Db, decidual basalis; Ch, chorion; MBS, maternal blood spaces; FC, fetal capillaries; LT, labyrinthine trophoblast. **P*<0.05, ***P*<0.01, ****P*<0.005 (Student's *t*-test). Error bars indicate s.d.

Development (2015) 142, 2425-2430 doi:10.1242/dev.121996

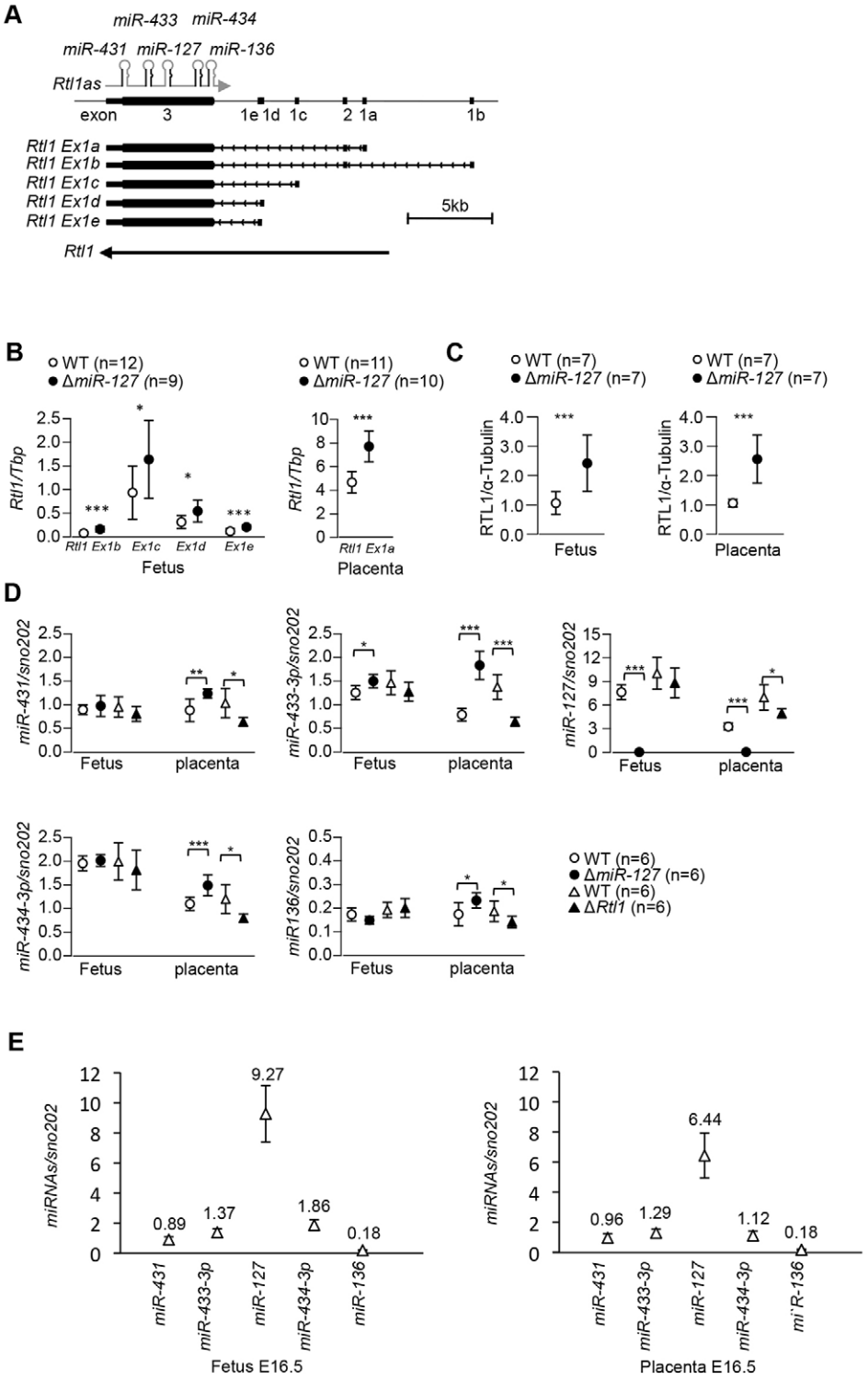

Fig. 3. Expression of *Rtl1* alternative transcripts and miRNAs in embryo and placenta at E16.5. (A) Structure of the mouse *Rtl1* locus. Alternative transcripts are transcribed from different leader exons. Exon 1s are named a-e. All alternative transcripts have a common exon 3 that has a conserved retrotransposon sequence. *Rtl1 Ex1a* and *Ex1b* also have a common exon 2. Exons are represented by a solid box. (B) Quantitative expression analysis for each alternative *Rtl1* transcript in Δ*miR-127* embryo and placenta at E16.5. (C) Western blotting for RTL1 normalised to α-tubulin in Δ*miR-127* embryo and placenta at E16.5. (D) miRNA expression is shown normalised to *snoRNA202*. (E) The relative expression of miRNAs. *miR-127* is the most abundant of the miRNAs in *Rtl1as*. **P*<0.05, ***P*<0.01, ****P*<0.005 (Student's *t*-test). Error bars indicate s.d.

angiogenesis, the degradation of the basement membrane and ECM facilitates migration into the interstitial matrix and the formation of new capillaries (Jain, 2003). Since placental Lz RTL1 protein is expressed in the capillary endothelial cells (Sekita et al., 2008), we propose that RTL1 promotes cleavage of the basement membrane to progress the vascularisation of FCs.

All *Rtl1* isoforms are regulated by *miR-127*

cDNA screening previously revealed that *Rtl1* has two exons and a transcription start site located 5 kb upstream of the retrotransposon-like sequences (Hagan et al., 2009), suggesting that *Rtl1* might be regulated by a host-derived promoter outside the retrotransposon. In order to clarify *Rtl1* transcript structure, we identified further *Rtl1* transcription start sites by 5′RACE. One alternative leader exon was identified in E15.5 placenta (*Rtl Ex1a*) and three alternatives were identified in the E11 embryo (*Rtl1 Ex1b*, *Ex1d* and *Ex1e*) (Fig. 3A; supplementary material Fig. S4). All five *Rtl1* alternative transcripts, including the known *Rtl1 Ex1c* (GenBank: EU434918), contain a common large exon, namely exon 3, which contains the retrotransposon-derived ORF, and different small exons. All

Development (2015) 142, 2425-2430 doi:10.1242/dev.121996

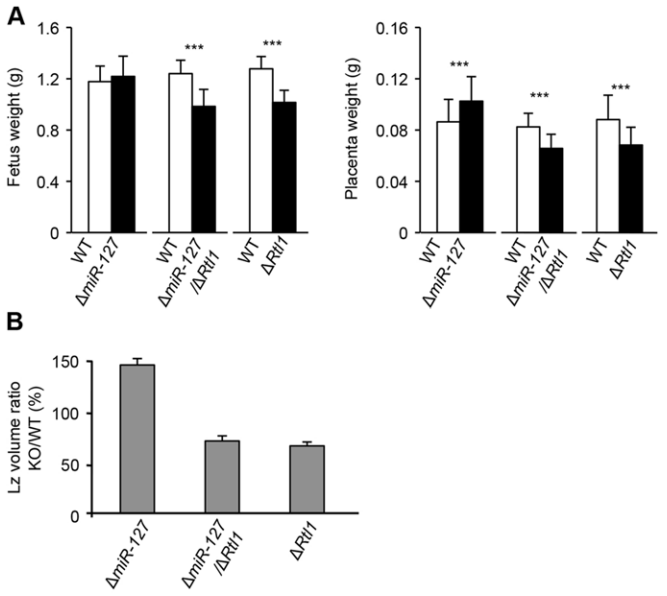

Fig. 4. Δ*miR-127*/Δ*Rtl1* knockout mice are comparable to Δ*Rtl1*. Double-heterozygous mice carrying both Δ*miR-127* and Δ*Rtl1* were born from heterozygous parents. (A) Fetal and placental weights at E18.5. (B) Volume ratio of the placental Lz at E18.5. ***P<0.005 (Student's t-test). Error bars indicate s.d.

alternative exon 1s are spread over a 12 kb region, suggesting that they might be transcribed from different promoters. To address this, real-time RT-PCR was performed using alternative transcript-specific forward primers and a common reverse primer in exon 3. This showed that *Rtl1 Ex1c* is the most abundant transcript in E16.5 whole embryos (supplementary material Fig. S3B). The other *Rtl1* transcripts were also detectable in E16.5 embryos, but the *Rtl1 Ex1a* expression level was much lower (0.6% of total) than for the other four. Conversely, the most abundant mRNA in the placenta was *Rtl1 Ex1a*, which contributed more than 97% of total *Rtl1* expression compared with the others (supplementary material Fig. S3B).

In order to address whether all *Rtl1* transcripts were equivalently modulated by *miR-127*, we quantified *Rtl1* transcript levels in Δ*miR-127* embryos and placentae. Results showed that all alternative transcripts were significantly overexpressed (~1.7-fold of control) in E16.5 Δ*miR-127* embryos (Fig. 3B). *Rtl1 Ex1a* was significantly increased (1.7-fold) in Δ*miR-127* placentae (Fig. 3B). This is not an indirect effect caused by a disproportionate increase in the number of endothelial cells, since there is a similar increase of 70% in *Ex1a* expression when normalised to the endothelial cell marker *Pecam1* (*CD31*) (supplementary material Fig. S3C). Analysis of hybrid fetuses and placentae showed that all alternative transcripts are exclusively transcribed from the paternal chromosome in Δ*miR-127* (supplementary material Fig. S3D), indicating that the overexpression is not associated with LOI. Western blotting showed that RTL1 protein was significantly increased and in proportion to the increased level of the transcript in E16.5 Δ*miR-127* embryos and placentae (Fig. 3C; supplementary material Fig. S1H). Since deletion of six of the seven miRNAs results in only a 2.5-fold increase in *Rtl1* mRNA (supplementary material Fig. S3E), our findings indicate that, compared with the other miRNAs in the cluster, *miR-127* contributes a proportionately greater effect on *Rtl1* levels in placentae, and disruption of this repression causes placental overgrowth.

Consistent with its impact on *Rtl1* levels, *miR-127* is the most abundant miRNA generated from *Rtl1as* (Fig. 3E). We next determined whether the deletion of *miR-127* influences expression of the neighbouring miRNAs to potentially impact *Rtl1* expression. As expected, *miR-127* was not detected in Δ*miR-127* embryos and placentae (Fig. 3D). In Δ*miR-127* fetuses, only *miR-433-3p* was upregulated, with no change in *miR-431*, *miR-434-3p* and *miR-136* expression (Fig. 3D). By contrast, all four miRNAs were significantly upregulated, with *miR-433-3p* the most induced, in Δ*miR-127* placenta. The same miRNAs that were upregulated in the placenta in the Δ*miR-127* mutant were downregulated in Δ*Rtl1* (Fig. 3D). Together, these results suggest that there might be a compensatory feedback mechanism involving RTL1 that acts specifically in the placenta to minimise the impact on *Rtl1* transcript levels. *miR-433* has its own promoter and thus might be more sensitive to this feedback mechanism (Song and Wang, 2008).

Rtl1 is the main target gene of *miR-127* for placenta development

Our data suggest *miR-127* can regulate placental growth through *Rtl1* repression. However, to address the possibility that other target genes of *miR-127* might also contribute to placental development, we generated double-heterozygous mice (Δ*miR-127*/Δ*Rtl1*) lacking both *Rtl1* and *miR-127*. If *Rtl1* is the main target of *miR-127* leading to repressed placental growth then the Δ*miR-127*/Δ*Rtl1* mutant should show a similar phenotype to Δ*Rtl1*. However, if *miR-127* has other targets contributing to this phenotype then the Δ*miR-127*/Δ*Rtl1* mutant would be expected to have an intermediate phenotype between that seen in Δ*Rtl1* and that seen in Δ*miR-127*. The Δ*miR-127*/Δ*Rtl1* mutant mouse embryo and placental weight data show that they are similar to Δ*Rtl1* at E18.5 rather than to Δ*miR-127* (Fig. 4A). Histological analysis also showed that the extent and volume reduction of the placental Lz was the same in both Δ*miR-127*/Δ*Rtl1* and Δ*Rtl1* (Fig. 2C and Fig. 4B). Detailed analysis of the Lz also determined that volumes and surface areas of the MBS, FC and LT and the TDC and SDC were similarly decreased in Δ*Rtl1* and Δ*miR-127*/Δ*Rtl1* compared with WT (supplementary material Table S3). By contrast, these volumes were increased in Δ*miR-127*. These striking similarities between Δ*Rtl1* and Δ*miR-127*/Δ*Rtl1* placentae suggest that *miR-127* specifically acts upstream of *Rtl1* during placental development.

Comparative analysis of the genomic locus between eutherian, metatherian and protherian mammals suggests that miRNAs on *Rtl1as* evolved in eutherians along with the neofunctionalisation of RTL1 (Edwards et al., 2008). Marsupial mammals lack the miRNAs and have retained only remnants of the Ty3/Gypsy retrotransposon that evolved into *Rtl1* in eutherians. Hence, it is likely that *Rtl1as* miRNAs evolved as a host defence mechanism to suppress the activity of this retrotransposon-derived gene (Edwards et al., 2008). In particular, the reciprocally imprinted *miR-127* and *Rtl1*, which interact so effectively in trans, co-evolved to regulate placenta development.

MATERIALS AND METHODS

Generation of Δ*miR-127*/Δ*Rtl1* mice

We generated a *miR-127* deletion construct that lacks 134 bp incorporating *miR-127* (chr12:109,592,803-109,592,936) (supplementary material Fig. S1A). The *miR-127* targeting construct was transfected into female 129SV ESCs and clones containing the targeting vector were selected (supplementary material Fig. S1C-E). After deletion of the neomycin resistance gene (supplementary material Fig. S1F), targeted ESCs were injected into blastocysts to make chimaeras and germline transmission confirmed. Animals were backcrossed to C57BL/6J for ten generations with consistent growth and viability phenotypes noted after N5 on this genetic background (supplementary material Table S1). Mice were subsequently maintained on a C57BL/6J genetic background. For further details, see the supplementary Materials and Methods.

Development (2015) 142, 2425-2430 doi:10.1242/dev.121996

Placental histology

Placentae from embryonic day (E) 18.5 conceptuses were dissected free of fetal membranes, weighed and bisected mid-sagittally. One half was fixed in 4% paraformaldehyde, paraffin embedded, sectioned, stained with Hematoxylin and Eosin (H&E) and the gross placental structure analysed. The other half was fixed in 4% glutaraldehyde, resin embedded, stained with Toluidine Blue and the structure stereologically assessed. Analyses were performed using the Computer Assisted Stereological Toolbox (CAST v2.0) program as previously described (Coan et al., 2004). Further details of placental histology are given in the supplementary Materials and Methods.

Rapid amplification of cDNA ends (5′RACE) and quantitative RT-PCR

5′RACE was performed using the First Choice RLM-RACE Kit (Ambion) following the manufacturer's protocol; 10 µg of total RNA from E11 fetus and E15.5 placenta was used as the starting material.

For real-time PCR, total RNA (10 µg) from whole embryos and placenta at E16.5 was treated with RQ1 RNase-free DNase (Promega). cDNA was synthesized using RevertAid H Minus First Strand cDNA Synthesis Kit with random hexamers (Fermentas). Real-time RT-PCR assay for *Rtl1* was performed using alternative exon 1-specific forward primers and a common reverse primer on exon 3. TATA box binding protein (*Tbp*) and *Pecam1* (*CD31*; Wang et al., 2005) expression was used as an internal control.

For mature miRNA expression, we carried out real-time RT-PCR using TaqMan microRNA assays (Applied Biosystems). Additional details of 5′ RACE and real-time RT-PCR are provided in the supplementary Materials and Methods.

Western blotting

Proteins were extracted from E16.5 embryos and placentae using RIPA buffer containing protease inhibitors (Complete, EDTA-free, Roche). RTL1 was detected by rabbit anti-RTL1 antibody (YZ2844) created in the C.L.S. laboratory, and then normalised by anti-α-tubulin (Sigma-Aldrich, T6199). Further details are given in the supplementary Materials and Methods.

Acknowledgements

We thank members of the A.C.F.-S. laboratory for discussions; and Neil Youngson, Simao Teixeira da Rocha, Sylvia Kocialkowski, Marika Charalambous and Marie Watkins for assistance and discussions during the course of this work.

Competing interests

The authors declare no competing or financial interests.

Author contributions

M.I. and A.C.F.-S. designed the study. M.I., A.N.S.-P., C.A.E., T.-H.L. and M.K. performed experiments. M.I., A.N.S.-P., S.E.A., T.K.-I., F.I., C.L.S. and A.C.F.-S. analysed and discussed the data. M.I., A.N.S.-P., B.T.A. and A.C.F.-S. wrote the manuscript.

Funding

This work was supported by the Biotechnology and Biological Sciences Research Council (BBSRC) and UK Medical Research Council (MRC) [MR/J001597/1] and EU FP7 Marie Curie Action 290123 (INGENIUM). This work was partly funded by a Australian Government National Health and Medical Research Council (NHMRC) CJ Martin Biomedical Fellowship to A.N.S.-P. Deposited in PMC for release after 6 months.

Supplementary material

Supplementary material available online at
http://dev.biologists.org/lookup/suppl/doi:10.1242/dev.121996/-/DC1

References

Brandt, J., Schrauth, S., Veith, A.-M., Froschauer, A., Haneke, T., Schultheis, C., Gessler, M. Leimeister, C. and Volff, J.-N. (2005). Transposable elements as a source of genetic innovation: expression and evolution of a family of retrotransposon-derived neogenes in mammals. *Gene* **345**, 101-111.

Ciaudo, C., Servant, N., Cognat, V., Sarazin, A., Kieffer, E., Viville, S., Colot, V., Barillot, E., Heard, E. and Voinnet, O. (2009). Highly dynamic and sex-specific expression of microRNAs during early ES cell differentiation. *PLoS Genet.* **5**, e1000620.

Coan, P. M., Ferguson-Smith, A. C. and Burton, G. J. (2004). Developmental dynamics of the definitive mouse placenta assessed by stereology. *Biol. Reprod.* **70**, 1806-1813.

da Rocha, S. T., Edwards, C. A., Ito, M., Ogata, T. and Ferguson-Smith, A. C. (2008). Genomic imprinting at the mammalian Dlk1-Dio3 domain. *Trends Genet.* **24**, 306-316.

Davis, E., Caiment, F., Tordoir, X., Cavaillé, J., Ferguson-Smith, A., Cockett, N., Georges, M. and Charlier, C. (2005). RNAi-mediated allelic trans-interaction at the imprinted Rtl1/Peg11 locus. *Curr. Biol.* **15**, 743-749.

Edwards, C. A., Mungall, A. J., Matthews, L., Ryder, E., Gray, D. J., Pask, A. J., Shaw, G., Graves, J. A. M., Rogers, J.; **SAVOIR consortium**, et al. (2008). The evolution of the DLK1-DIO3 imprinted domain in mammals. *PLoS Biol.* **6**, e135.

Ferguson-Smith, A. C. (2011). Genomic imprinting: the emergence of an epigenetic paradigm. *Nat. Rev. Genet.* **12**, 565-575.

Gundersen, H. J. G., Bendtsen, T. F., Korbo, L., Marcussen, N., Møller, A., Nielsen, K., Nyengaard, J. R., Pakkenberg, B., Sørensen, F. B., Vesterby, A. et al. (1988). Some new, simple and efficient stereological methods and their use in pathological research and diagnosis. *APMIS* **96**, 379-394.

Hagan, J. P., O'Neill, B. L., Stewart, C. L., Kozlov, S. V. and Croce, C. M. (2009). At least ten genes define the imprinted Dlk1-Dio3 cluster on mouse chromosome 12qF1. *PLoS ONE* **4**, e4352.

Iorio, M. V., Ferracin, M., Liu, C.-G., Veronese, A., Spizzo, R., Sabbioni, S., Magri, E., Pedriali, M., Fabbri, M., Campiglio, M. et al. (2005). MicroRNA gene expression deregulation in human breast cancer. *Cancer Res.* **65**, 7065-7070.

Jain, R. K. (2003). Molecular regulation of vessel maturation. *Nat Med.* **9**, 685-693.

Laga, E. M., Driscoll, S. G. and Munro, H. N. (1973). Quantitative studies of human placenta. I. Morphometry. *Biol. Neonate.* **23**, 231-259.

Lin, S.-P., Youngson, N., Takada, S., Seitz, H., Reik, W., Paulsen, M., Cavaille, J. and Ferguson-Smith, A. C. (2003). Asymmetric regulation of imprinting on the maternal and paternal chromosomes at the Dlk1-Gtl2 imprinted cluster on mouse chromosome 12. *Nat. Genet.* **35**, 97-102.

Lu, J., Getz, G., Miska, E. A., Alvarez-Saavedra, E., Lamb, J., Peck, D., Sweet-Cordero, A., Ebert, B. L., Mak, R. H., Ferrando, A. A. et al. (2005). MicroRNA expression profiles classify human cancers. *Nature* **435**, 834-838.

Mandarim-de-Lacerda, C. A. (2003). Stereological tools in biomedical research. *An. Acad. Bras. Cienc.* **75**, 469-486.

Riordan, J. D., Keng, V. W., Tschida, B. R., Scheetz, T. E., Bell, J. B., Podetz-Pedersen, K. M., Moser, C. D., Copeland, N. G., Jenkins, N. A., Roberts, L. R. et al. (2013). Identification of *Rtl1*, a retrotransposon-derived imprinted gene, as a novel driver of hepatocarcinogenesis. *PLoS Genet.* **9**, e1003441.

Seitz, H., Youngson, N., Lin, S.-P., Dalbert, S., Paulsen, M., Bachellerie, J.-P., Ferguson-Smith, A. C. and Cavaillé, J. (2003). Imprinted microRNA genes transcribed antisense to a reciprocally imprinted retrotransposon-like gene. *Nat. Genet.* **34**, 261-262.

Sekita, Y., Wagatsuma, H., Nakamura, K., Ono, R., Kagami, M., Wakisaka, N., Hino, T., Suzuki-Migishima, R., Kohda, T., Ogura, A. et al. (2008). Role of retrotransposon-derived imprinted gene, Rtl1, in the feto-maternal interface of mouse placenta. *Nat. Genet.* **40**, 243-248.

Song, G. and Wang, L. (2008). MiR-433 and miR-127 arise from independent overlapping primary transcripts encoded by the miR-433–127 locus. *PLoS ONE* **3**, e3574.

Wang, H., Riha, G. M., Yan, S., Li, M., Chai, H., Yang, H., Yao, Q. and Chen, C. (2005). Shear stress induces endothelial differentiation from a murine embryonic mesenchymal progenitor cell line. *Arterioscler. Thromb. Vasc. Biol.* **25**, 1817-1823.

Youngson, N. A., Kocialkowski, S., Peel, N. and Ferguson-Smith, A. C. (2005). A small family of sushi-class retrotransposon-derived genes in mammals and their relation to genomic imprinting. *J. Mol. Evol.* **61**, 481-490.

Supplementary materials and methods

Mice

We generated a *miR-127* deleted construct with the neomycin resistance gene (Fig. S1A). Three large genomic DNA fragments were amplified by PCR using KOD HiFi DNA polymerase (Novagen) (Fragment A: chr12:109,590,618-109,595,291, Fragment B: chr12:109,595,397-109,597,519, Fragment C: chr12:109,597,500-109,599,896 respectively, from the mouse reference genome mm9 assembly (Fig. S1A). These fragments were independently cloned into the TOPO cloning vector (Invitrogen). *miR-127* was removed from fragment A by *Ava*I digestion (chr12:109,592,803-109,592,936). Cloned fragments were combined into the neoflox8 vector (provided by U. Lichtenberg, Cologne) including the neomycin resistance gene. The small gap between fragment A and fragment B was filled with a small PCR fragment. After G418 selection followed by transfection of the *miR-127* targeting construct into female 129Sv ES cells, the recombinants were screened by PCR and Southern blotting (Fig. S1B-D). The primers for screening are (short arm) neof1077F 5'-CGCCAATGACAAGACGCTGG and pEX1R 5'-CGTCTGCATGACCTAGAGGC. Primers for screening the miR127 deletion are Rtl1 9486R 5'-ACCTGGCCGACGTGTTTA and AW060F 5'-CCGAACGATGCTCTCCAAGTG. Targeted ES Cells were treated with *Cre* recombinase to delete the neomycin resistance gene (Fig. S1E). The primers for screening the loxP deletion are Rtl1 13940 5'-ATTTGCAGCAATCCGATTTT and Rtl1 14143 5'-TGTCTGTGTATGTGAATATGTGTGC. ES targeting and blastocyst injection was carried out by the Gene Targeting Facility at The Babraham Institute. Mice were crossed into and maintained on a C57BL/6J genetic background unless otherwise indicated. For allelic expression analysis, hybrid conceptuses were

made from Δ*miR-127* female mated with WT congenic male carrying *Dlk1-Dio3* cluster from *Mus musculus molossinus*. Experiments involving mice were carried out in accordance with the UK Government Home Office licensing procedures (licence 80/2567).

Placental histology

Dissected placentae were cut mid-sagittally and one half was fixed in 4% paraformaldehyde in 70 mM phosphate buffer and the other half fixed in 4% glutaraldehyde in Pipes buffer. Following fixation, the paraformadehyde-fixed half was dehydrated, embedded in paraffin wax, sectioned at 7µm and stained with haematoxylin and eosin. The glutaraldehyde-fixed half was dehydrated and embedded in Spurr epoxy resin (Taab, Aldermaston, UK) and a 1 µm vertical section cut close to the placental midline was stained with Toluidine Blue. Paraffin and resin embedded sections were analyzed using superimposed grids and systematic sampling within random fields and the Computer Assisted Stereological Toolbox (CAST v2.0). The proportion of placental compartments; the labyrinthine zone, junctional zone and decidua were determined by point counting on the haematoxylin and eosin sections and then converted into estimated volumes by multiplying their proportion by total placental weight. Labyrinthine morphometric analyses were performed on resin sections as described by Coan et al., 2004.

Rapid Amplification of cDNA Ends (5'RACE)

5'RACE was performed using First Choice® RLM-RACE (Ambion) using 10 µg of total RNA from E11 embryo and E15.5 placenta. Standard reactions were performed following the manufacturer's protocol. For first round synthesis each 25 µl reaction

contained 1X PCR buffer (KOD Hot Start, Novagen), 300 µM dNTPs, 1 mM $MgSO_4$, 0.5 U Hot Start KOD polymerase, 0.4 µM of each primer (5'RACE Outer primer and 11545F 5'-CAGTGGGCAGCTCTTGCATTTCCTG) and 1-2 µl RT reactions. The PCR cycling program was: 94ºC for 3 minutes, then 35 cycles at 94ºC for 30 seconds, 58ºC for 30 seconds, 72ºC for 2 minutes and a 7 minute extension cycle at 72ºC. The second round of PCR was performed as above using 1-2 µl of the first round PCR as the template. In this reaction the 5'RACE inner primer and RRACE1 5'-TGTCGTCGGTTGGAAAGGAGTGTGC were used. The products were cloned into pGEM-T easy (Promega) and sent for Sanger sequencing.

Real time RT-PCR

Total RNA was extracted from whole embryos and placenta at E16.5 using TRI Reagent (Ambion). Reactions were run in 12.5 µl in the presence of 1× SYBR Green JumpStart *Taq* ReadyMix (Sigma Aldrich), 400 nM primers. PCR conditions were 95°C for 15 min followed by 40 cycles at 95°C for 15 seconds, 66°C for 30 seconds and 72°C for 5 seconds on a DNA Engine OPTICON2 (MJ Research). All reactions were performed in triplicate. The primers used were as follows: Forward primer Rtl1Ex1aF 5'-CAAGGACTCTCCCTCTCCAC, Rtl1Ex1bF 5'-AGGCACCCGAGCAGAGAG, RtlEx1cF 5'-GCTCAGAGGCAATCAAGGAG, Rtl1Ex1dF 5'-GAAGGCACT-ATTGCATCCTGA, Rtl1Ex1eF 5'-AGTTTGGCCAAGGAAGGATT, Reverse primer RRACE1 5'-TGTCGTCGGTTGGAAAGGAGTGTGC. For reference, Tbp F 5'-GGCCTCTCAGAAGCATCACTA, Tbp R 5'-AGGCCAAGCCCTGAGCATAA or Pecam1 F 5'-TCCCTGGGAGGTCGTCCAT, Pecam1 R 5'-GAACAAGGCAGCGGGGTTTA (Wang et al., 2005).

For direct comparison of *Rtl1* expression levels between the Δ*miR-127* and the maternally inherited multi-microRNA deletion (Sekita et al., 2008). cDNAs were synthesised from both mutant placentae using SuperScriptIII according to the method described previously (Sekita et al, 2008). Reactions were run in 10 µl in the presence of 1× SYBR Green I Master (Roche), 400 nM primers. PCR conditions were 95°C for 5 min followed by 45 cycles at 95°C for 10 seconds, 66°C for 10 seconds and 72°C for 10 seconds on LightCycler 480 II (Roche). The primers, Rtl1Ex1aF and RRACE1, Tbp F and Tbp R, were used for *Rtl1 Ex1a* and *Tbp* analysis, respectively.

For allelic-specific expression analysis, five forward primers, Rtl1Ex1aF to Rtl1Ex1eF, and reverse primer RRACE8 5'-ACTTCTTGGAGTAGATTAGTGGGCAGCTC were used. The amplicons were gel purified using MinElute Gel Extraction Kit (Qiagen) and SNP (rs242380595) was detected by direct sequencing.

For mature miRNAs, we used TaqMan MicroRNA assays (Life technologies). *miR-127* (mmu-miR-127, 4427975-001183), *miR-431* (hsa-miR-431, 4427975-001979), *miR-433* (has-miR-433, 4427975-001028) *miR-434-3p* (mmu-miR-434-3p, 4427975-001140) and *miR-136* (mmu-miR-136, 4427975-002511), accumulation was monitored and *snoRNA202* (snoRNA202, catalog number; 4427975-001232) was used as standard internal control. First strand cDNA was synthesized from total RNA from embryo and placenta using RevertAid H minus First Strand cDNA synthesis kit (Fermentas). Briefly, multiplex reverse transcription was carried out with 10ng total RNA, 0.5mM dNTPs, 120unit M-MuLV reverse transcriptase, four TaqMan miRNA RT primers mix (0.65 µl each) and 1 x RT buffer in 6 µl reaction mix with 10 µl mineral oil overlay. The reverse transcription reaction consisted of 30 min at 16˚C, 30 min at 42˚C and 5 min at 85˚C. Real time PCR was carried out using TaqMan

Universal Master Mix, No AmpErase UNG (Applied Biosystems) following the manufacture's instructions. Signals were detected using the ABI Fast real time PCR Systems (Applied Biosystems) and quantification carried out by the comparative Ct method. Experiments were repeated in triplicate.

Western blotting

Proteins were isolated from E16.5 embryos and placentae. Ten micrograms of protein were separated by 6% SDS-PAGE and then blotted to PVDF membranes. After incubation with 5% skimmed milk in 0.1% PBST for 60 min, the membrane was washed three times with 0.1% PBST and incubated with antibodies against RTL1 (1:1000) or α-Tublin (1:10000, Sigma Aldrich, T6199). Membranes were washed three times for 10 min and incubated with a 1:2000 dilution of HRP conjugated anti-rabbit or anti-mouse antibodies for 2h. Blots were washed with 0.1% PBST three times and developed with the ECL system (Amersham Biosciences) according to the manufacturer's protocol. The anti-RTL1 antibody (YZ2844) was produced by YenZym Antibodies, LLC (South San Francisco, CA). The RTL1 antigen (chr12:109,594,459-109,595,139) and His fusion protein was immunised in rabbits and the antibody was purified.

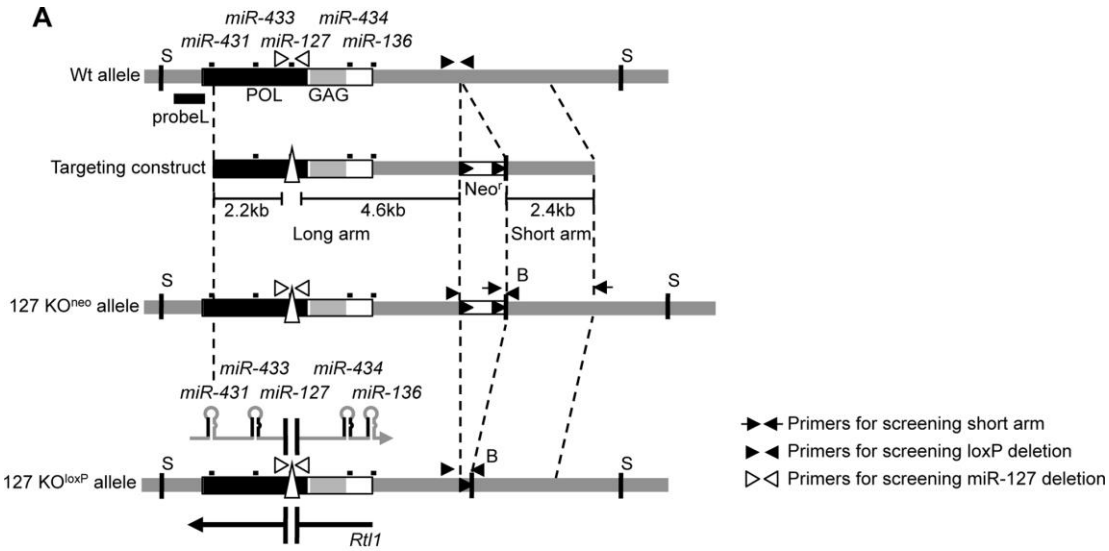
A
miR-433 miR-434
miR-431 miR-127 miR-136
Wt allele
S
POL
GAG
probeL
Targeting construct
Neo^r
2.2kb
4.6kb
2.4kb
Long arm
Short arm
B
127 KO^neo allele
127 KO^loxP allele
Rtl1
Primers for screening short arm
Primers for screening loxP deletion
Primers for screening miR-127 deletion

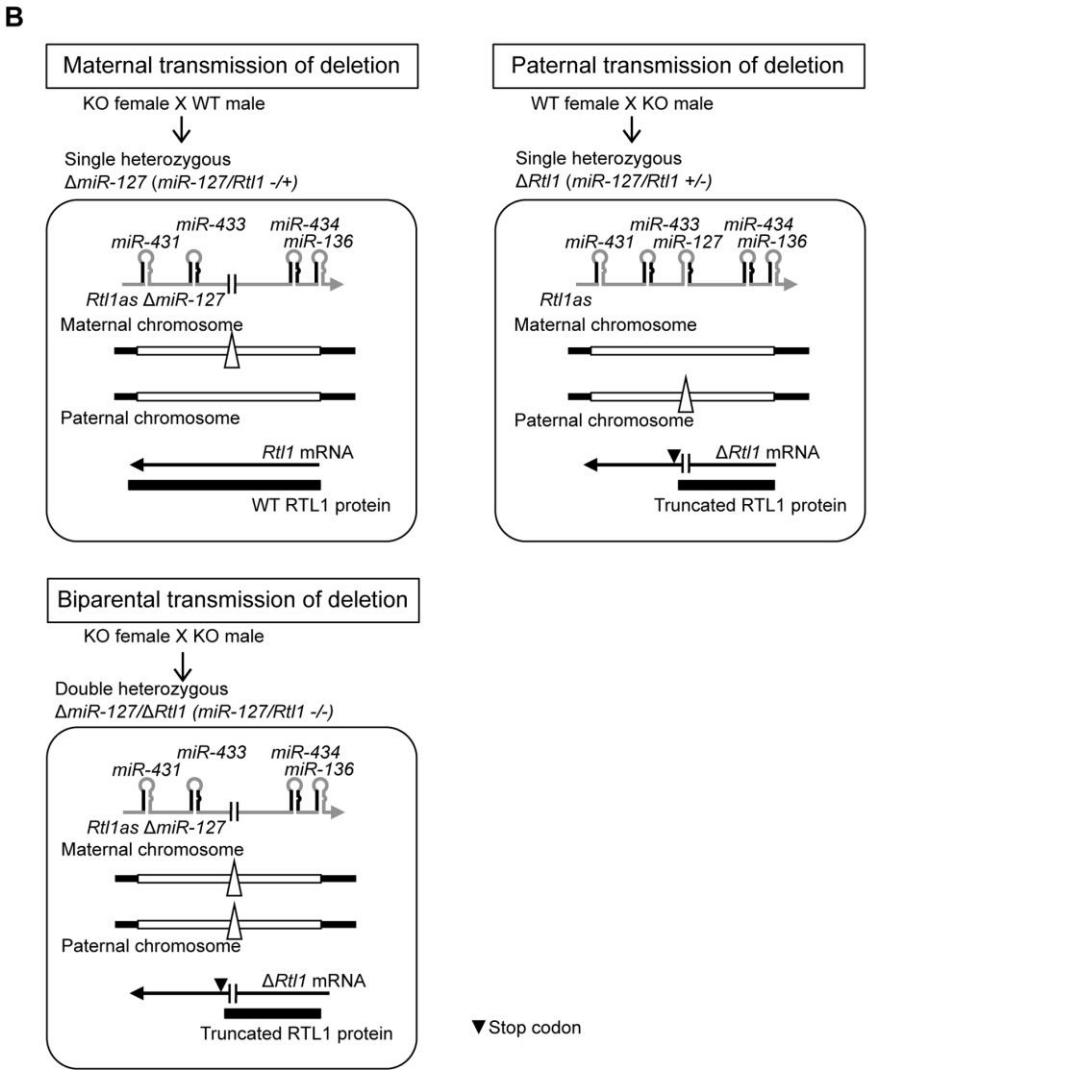
B
Maternal transmission of deletion
KO female X WT male
Single heterozygous
ΔmiR-127 (miR-127/Rtl1 -/+)
miR-433 miR-434
miR-431 miR-136
Rtl1as ΔmiR-127
Maternal chromosome
Paternal chromosome
Rtl1 mRNA
WT RTL1 protein
Paternal transmission of deletion
WT female X KO male
Single heterozygous
ΔRtl1 (miR-127/Rtl1 +/-)
miR-433 miR-434
miR-431 miR-127 miR-136
Rtl1as
Maternal chromosome
Paternal chromosome
ΔRtl1 mRNA
Truncated RTL1 protein
Biparental transmission of deletion
KO female X KO male
Double heterozygous
ΔmiR-127/ΔRtl1 (miR-127/Rtl1 -/-)
miR-433 miR-434
miR-431 miR-136
Rtl1as ΔmiR-127
Maternal chromosome
Paternal chromosome
ΔRtl1 mRNA
Truncated RTL1 protein
▼Stop codon

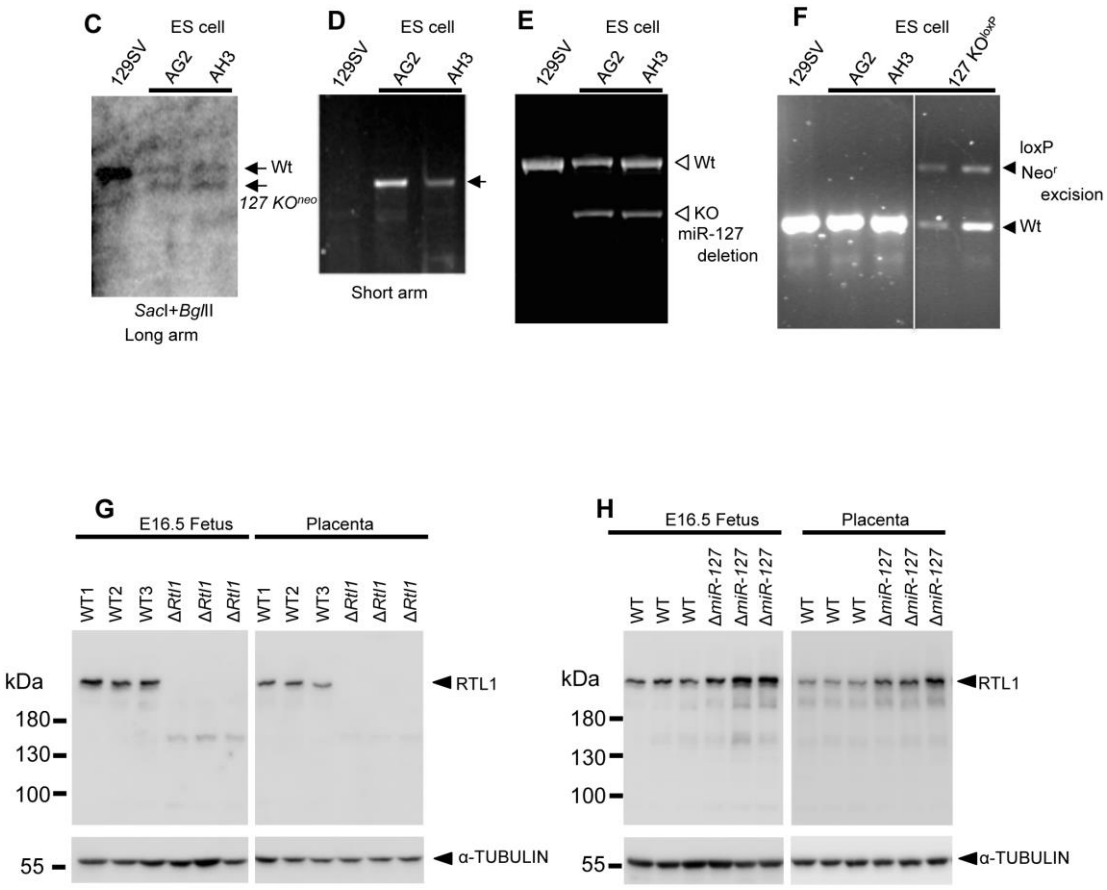

Fig. S1. Production of Δ*Rtl1* and Δ*miR-127* mice. (A) Schematic representation of the knockout strategy. The third exon of *Rtl1* is shown as an open box. Gag homology domains are shaded grey and Pol homology domains are black. LoxP sites are shown as solid triangles and the deleted site is indicated as an open triangle. *Sac*I [S] and *Bgl*II [B] restriction sites and probeL were used for recombinant screening the long arm of the targeted allele by Southern blotting. Three primer sets were used for PCR screening of the targeted allele. Arrowheads show primers for screening the short arm of the targeted allele, 127 KO^{neo}. The neomycin-resistance gene (*Neo^r*) was removed in ES cells by *Cre recombinase.* The solid arrow heads indicate primers for screening of the Neo^r excluded allele (*127 KO^{loxP}*). The open arrows are primers for screening for the *miR-127* deleted allele. (B) Single heterozygous and double heterozygous are indicated. The upper-left panel shows maternal transmission of the

small deletion. These single heterozygous mutant mice, *miR-127/Rtl1 -/+* lose *miR-127* expression. The upper-right panel shows reciprocal paternal transmission of the same deletion. Here, the small deletion makes *Rtl1* mRNA without the *miR-127* binding site. The deletion also induces a frame shift resulting in a nonsense mutation in the *Rtl1* ORF which would result in a truncated RTL1 protein. Hence, the single heterozygous mutant mice, *miR-127/Rtl1 +/-* lose functional RTL1 protein. The lower panel shows biparental transmission of the small deletion. These double heterozygous mutant mice, *miR-127/Rtl1 -/-* lose *miR-127* expression and functional RTL1 protein expression. (C) Southern blots of genomic DNA for screening for long arm recombination. Southern blots of genomic DNA from ES cells that have WT alleles (left; 129Sv), and *127 KO*^{neo} allele (middle; AG2 and right; AH3). (D) PCR screening for the short arm of the *127 KO*^{neo} allele. The left lane shows WT (no signal) and the middle and right lanes indicate *127 KO*^{neo} alleles. (E) PCR results show the *miR-127* deleted allele (lower signal) and WT allele (upper signal) in 129Sv, AG2 and AH3 ES cells. (F) After *Cre recombinase* treatment, PCR shows the WT allele (lower signal) and the *Neo*^{r} deleted allele (upper signal). The *Neo*^{r} inserted allele is not detected by PCR. (G) Western blotting shows that Δ*Rtl1* embryos and placentae lacked RTL1 protein expression. The premature truncated RTL1 protein cannot be observed in predicted size (95.6 kDa) in both Δ*Rtl1* embryos and placentae. (H) Western blotting shows Δ*miR-127* embryos and placentae with increased RTL1 protein expression.

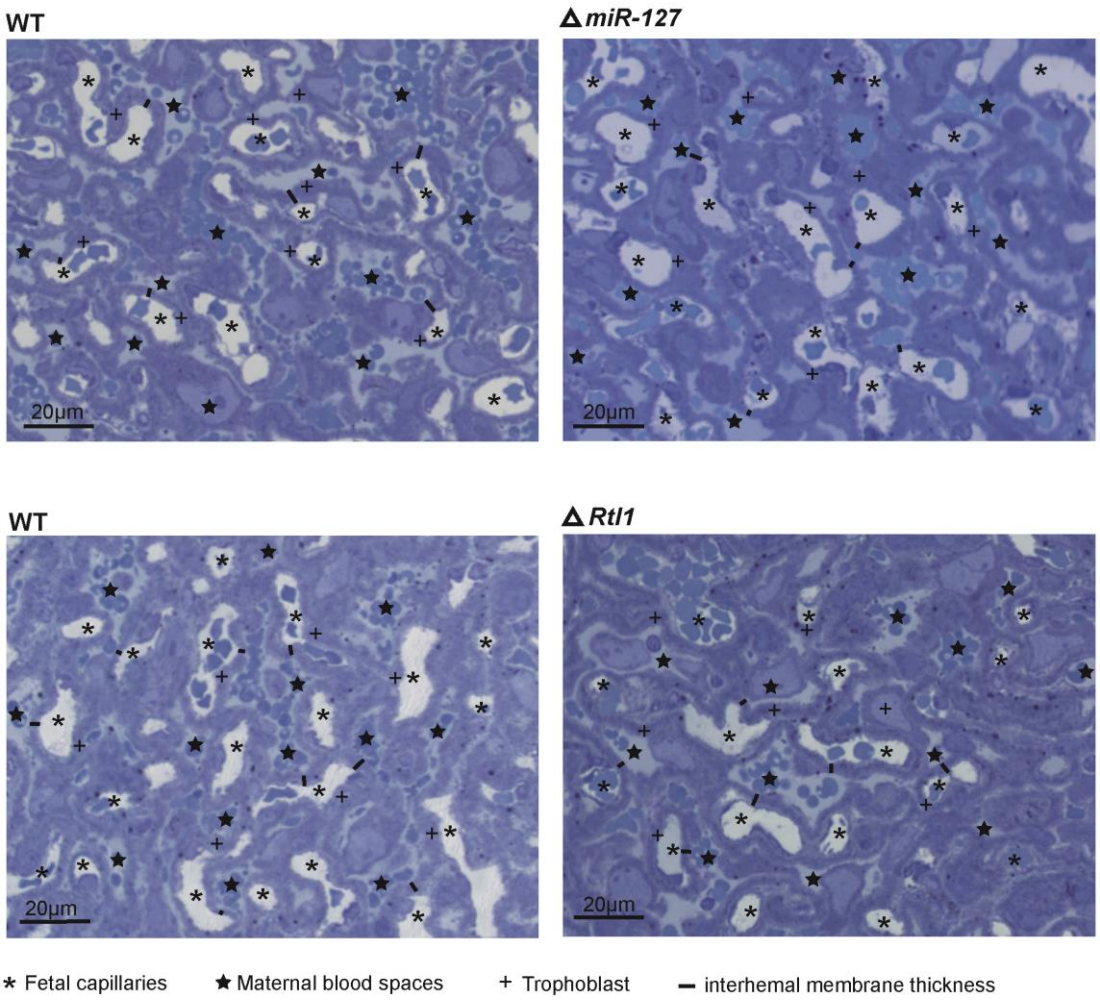

Fig. S2. Photomicrographs of placental labyrinthine zone. The photomicrographs show toluidine stained resin-embedded sections of E18.5 placentae. Fetal capillaries, trophoblast and maternal blood spaces from which the volume fractions, absolute volumes and surface areas and fetal capillary length can be derived as well as the interhemal membrane thickness (black bar) determined, using established, published stereological methods (Fig. 2E,F and table S3).

A

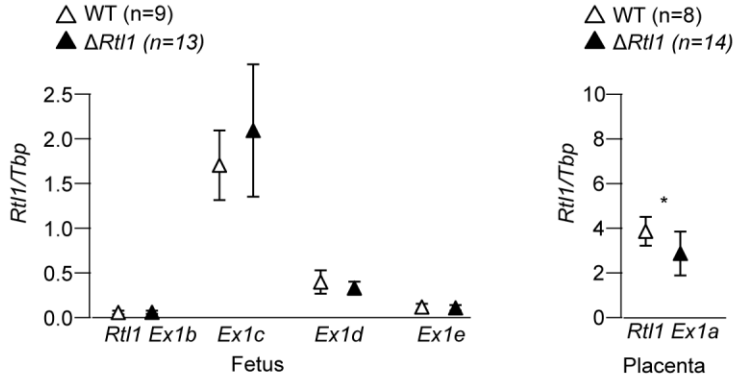

Student's t-test was used for statistic analysis . *** P<0.005

B

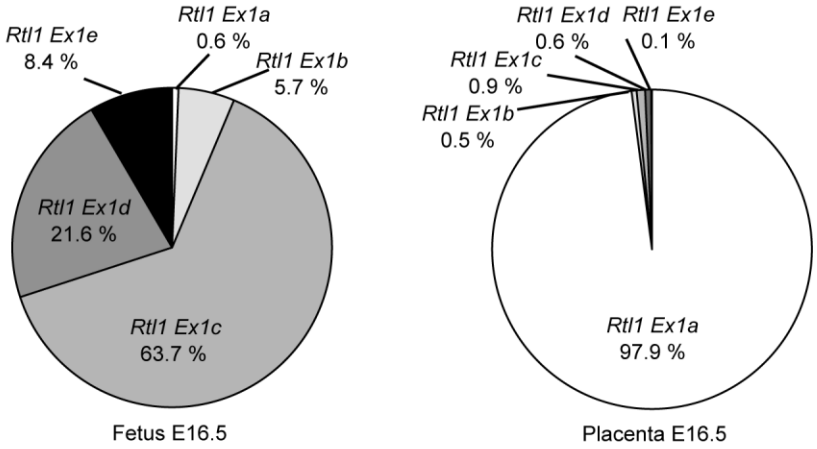

C

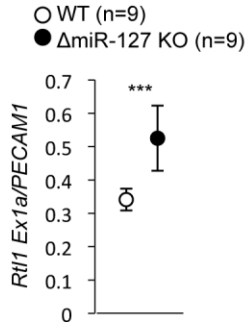

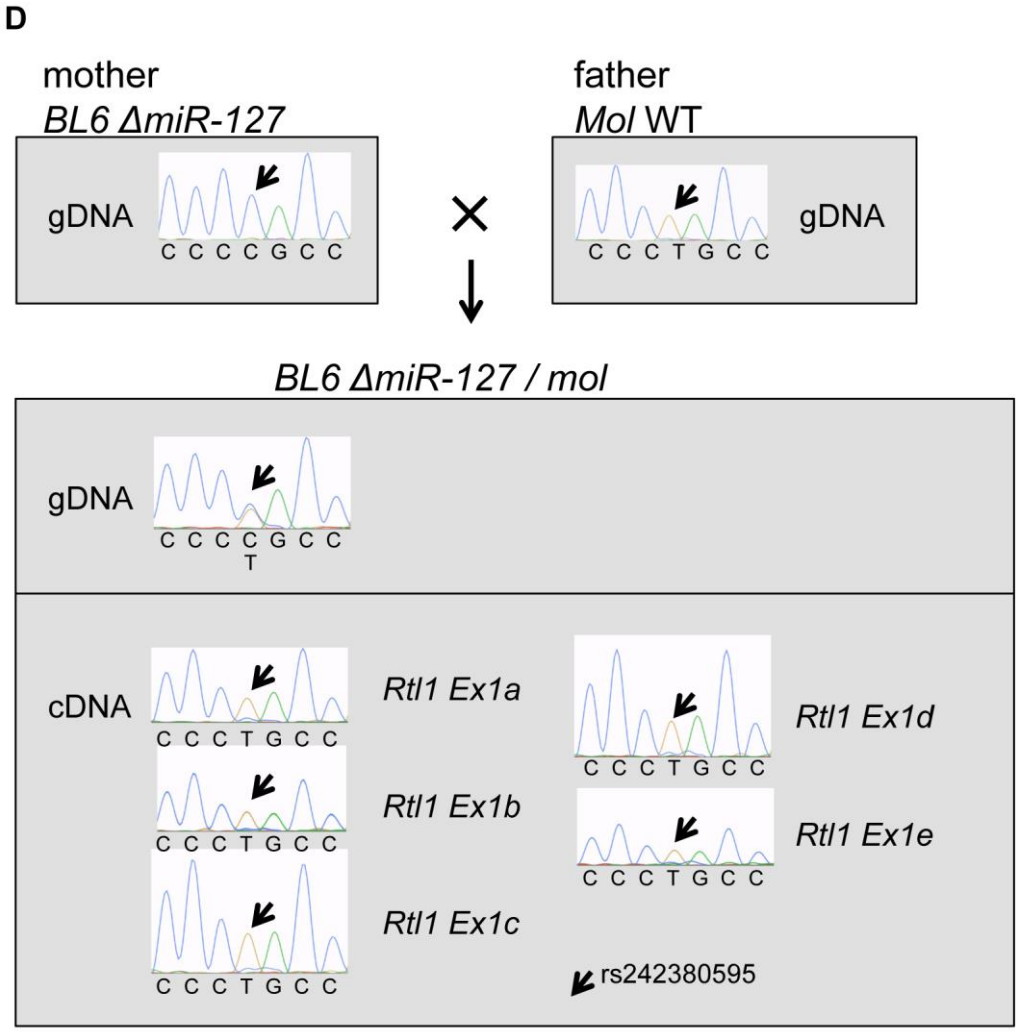

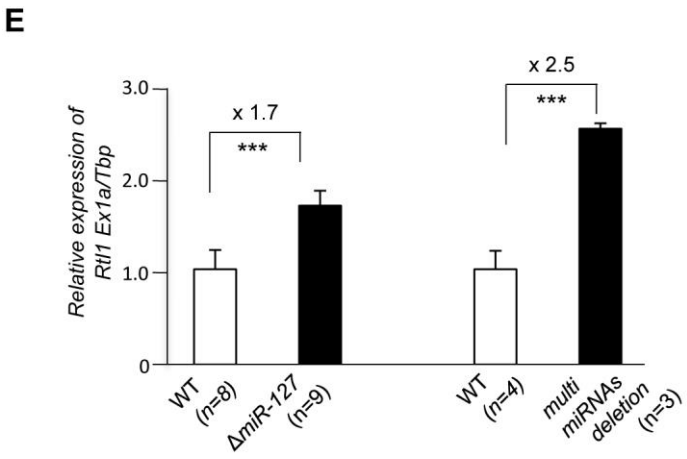

Fig. S3. Expression analysis for each alternative *Rtl1* transcript and the miRNAs. (A) As expected, the deleted *Rtl1* mRNAs were transcribed and stable in Δ*Rtl1*. There is no significant difference in *Rtl1* mRNAs between Δ*Rtl1* and WT embryos. In placenta, *Rtl1 Ex1a* expression was reduced slightly compared to WT.

Error bars represent s.d. Statistically significant differences are indicated by an asterisk (student's t-test; *; P<0.05). (B) Graphs indicate transcription level of each alternative transcript at E16.5 fetus and placenta. (C) Since the expression of *Rtl1 Ex1a* normalised to the endothelial cell marker *PECAM1/CD31* increased *in* Δ*miR-127* placenta, the expansion of endothelial cells does not cause the increase of *Rtl1 Ex1a.* (D) All five *Rtl1* alternative transcripts are exclusively transcribed from the paternal chromosome in Δ*miR-127*. (E) Quantitative expression analysis for the *Rtl1 Ex1a* transcript in Δ*miR-127* and the multi-miRNA deletion placentas (Sekita et al., 2008) at E16.5.

Fig. S4. The sequences of alternative *Rtl1* transcripts. The sequences of 5' RACE products are shown. Each box indicates alternative exon1 or exon2. Unboxed sequence represents the 5' end of exon3. *Rtl1 Ex1c* is reported in GeneBank database as EU434918. *Rtl1 Ex1a* was cloned from E15.5 placenta. The other three were cloned from E11 embryos.

Table S1 The lethality of the Δ*miR-127 and* Δ*Rtl1* mice.

Maternal Δ*miR-127*	WT	KO
N3	44	32
N4	24	23
N5	21	20
N6	78	82
N7	77	56
N8	51	51
N9	53	45
N10	19	15
>N11	150	154

The number of WT and Δ*miR-127* mice which grew to adulthood generation are shown. The Δ*miR-127* mice and WT mice have comparable survivability during backcrossing with C57BL/6J.

Paternal Δ*Rtl1*	WT	KO
N2	26	29
N4	8	8
N5	36	8*
N6	30	7*
N7	93	47*
N9	57	4*
N10	15	2*
N12	56	4*
N14	40	10*

The number of WT and Δ*Rtl1* mice which grew to adulthood generation are shown. The survivability of Δ*Rtl1* mice decreased during backcrossing with C57BL/6J. Pearson's chi-square test was used for statistic analysis (*; P<0.05)

Paternal Δ*Rtl1* (129aa X C57BL/6J hybrid background)

	WT	KO
N14	38	38

The number of WT and Δ*Rtl1* mice in 129aa X C57BL/6J hybrid background are shown. The 129aa background can rescue the lethality of the Δ*Rtl1* mice in N14 generation.

Supplemental Table S2 The survivability of Δ*miR-127 and* Δ*Rtl1* at embryonic stage.

Maternal Δ*miR-127*		KO/WT weight Ratio (%)	
Stage	WT:Δ*miR-127*	embryo	placenta
E12.5	9: 5	105.4	97.5
E14.5	16:21	102.3	101.1
E16.5	40:32	99.0	111.6*
E18.5	22:19	102.0	118.5*
Total	87:77		

Paternal Δ*Rtl1*		KO/WT weight Ratio (%)	
Stage	WT:Δ*Rtl1*	Fetus	placenta
E12.5	2: 1	82.7	106.1
E14.5	19:26	101.1	81.6*
E16.5	12:20	80.7*	82.2*
E18.5	31:21	79.5*	77.5*
Total	64:68		

Student's t-test was used for Statistic analysis * $p<0.05$

Supplemental Table S3. Stereological analysis of placentae from *miR-127* and *Rtl1* single or double homozygous knockout mice on E18.5.

	WT (N=4)	Δ*miR-127*/+ (N=3)	Δ*miR-127*/WT (%)	WT (N=6)	+/Δ*Rtl1* (N=4)	Δ*Rtl1*/WT (%)	WT (N=4)	Δ*miR-127*/ Δ*Rtl1* (N=7)	KO/WT (%)
Placental compartment volume; mm^3 (proportion; %)									
Lz	46.3±5.7 (51.7)	65.9±5.1** (57.7)	142.3	46.4±4.3 (55.3)	30.0±9.4*** (41.1)*	64.7	41.1±4.1 (49.9)	28.5±5.4*** (45.0)*	69.3
Jz	24.5±9.2 (26.9)	20.9±8.1 (17.7)	85.3	20.2±4.9 (23.9)	22.6±4.1 (31.3)*	111.9	23.6±3.8 (28.6)	19.0±4.9 (29.8)	80.5
Db	13.6±2.6 (15.4)	10.2±6.0 (9.6)	75.0	12.2±2.3 (14.7)	10.7±1.4 (15.1)	87.7	9.7±0.8 (11.8)	10.2±2.4 (16.3)*	105.2
Ch	5.4±1.2 (6.0)	18.6±14.2 (15.1)	344.4	5.1±2.9 (6.1)	9.2±4.0 (12.5)*	180.4	8.2±3.5 (9.8)	5.8±2.9* (8.9)*	70.7
Labyrinthine compartment volume; mm^3 (proportion; %)									
MBS	7.4±0.8 (16.5)	9.9±2.4 (15.0)	133.8	6.2±2.3 (13.3)	4.0±1.1 (13.7)	64.5	10.8±2.0 (26.2)	6.4±1.8** (22.8)	59.3
FC	6.5±1.5 (15.3)	12.3±2.7* (18.6)	189.2	7.3±1.3 (15.7)	3.3±1.7** (10.7)**	45.2	6.4±0.9 (15.6)	3.7±2.1*** (12.5)	57.8
LT	32.3±4.1 (68.2)	43.7±5.6* (66.4)	135.3	32.9±2.5 (71.0)	22.7±7.1** (75.6)	69.0	23.9±3.2 (58.2)	18.3±3.0** (64.7)	76.6
Theoretical diffusion capacity; $mm^2.min^{-1}.kPa^{-1}$									
	12.8±3.5	19.3±3.5*	150.3	14.5±2.5	9.1±3.6*	62.6	14.6±2.6	9.4±3.8***	64.2
Specific diffusion capacity; $mm^2.min^{-1}.kPa^{-1}.g$ fetus									
	11.6±2.7	16.8±1.0*	145.5	11.4±1.8	8.8±3.5	77.5	11.7±2.5	9.2±1.9**	78.1
Lz interhemal membrane surface areas; cm^2									
MBS	23.6±7.3	35.5±6.8*	150.4	35.6±3.9	23.8±9.6*	66.8	31.9±5.5	21.2±4.3***	66.5
FC	21.4±3.6	33.1±7.7*	154.7	21.0±3.9	14.3±4.7*	68.3	17.4±2.8	11.4±3.6***	65.4
mean	22.5±5.8	34.3±5.9*	152.4	28.3±3.7	19.0±7.1*	67.4	24.7±3.3	16.3±3.8***	66.1
Interhemal membrane harmonic mean thickness; µm									
T_h	3.2±0.1	3.2±0.1	100.3	3.4±0.4	3.6±0.1	106.7	2.9±0.3	3.2±0.6	107.0
Labyrinthine fetal capillaries									
Length (m)	112.0±21.4	184.2±11.9***	164.4	136.0±20.5	85.2±31.2**	62.6	113.1±32.1	79.6±15.3*	70.4
Diameter (µm)	9.2±0.7	8.2±1.0	90.0	7.5±1.4	8.4±1.0	111.9	11.2±0.9	10.2±1.6	91.1

Data are presented as mean±SD. Student's t-test was used for Statistic analysis * P>0.05, ** P>0.01, *** P>0.005.
Abbreviations: Lz, labyrinthine zone; Jz, junctional zone; Db, decidua basalis; Ch, chorion; MBS, maternal blood spaces; FC, fetal capillaries; LT, labyrinthine trophoblast.